

See discussions, stats, and author profiles for this publication at: <https://www.researchgate.net/publication/231376438>

Effects of O₂ on Characteristics of Sulfur Added to Petroleum Coke through Reaction with SO₂

ARTICLE *in* INDUSTRIAL & ENGINEERING CHEMISTRY RESEARCH · NOVEMBER 2010

Impact Factor: 2.59 · DOI: 10.1021/ie101388q

CITATIONS

6

READS

39

2 AUTHORS:



Eric Morris

University of Toronto

7 PUBLICATIONS 46 CITATIONS

[SEE PROFILE](#)



Charles Q Jia

University of Toronto

80 PUBLICATIONS 803 CITATIONS

[SEE PROFILE](#)

Effects of O₂ on Characteristics of Sulfur Added to Petroleum Coke through Reaction with SO₂

Eric A. Morris[†] and Charles Q. Jia*

Department of Chemical Engineering & Applied Chemistry, University of Toronto, 200 College Street, Toronto, Ontario, Canada, M5S 3E5

Kazuki Morita[‡]

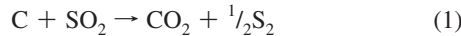
Institute of Industrial Science, University of Tokyo, 4-6-1, Komaba, Meguro-ku, Tokyo, 153-8505, Japan

Alberta oil-sands petroleum coke is an abundant byproduct of the upgrading of bitumen. The current study aims to improve the current understanding of sulfur added to the surface of petroleum coke through reaction with sulfur dioxide (SO₂) and how this is affected by a large excess of oxygen (O₂). Particular focus is given to the distribution and speciation of sulfur within the coke particles, as well as its thermal stability. Petroleum coke was activated in SO₂ with and without O₂ in a packed bed reactor at 600–800 °C. The activated cokes were characterized with electron probe microanalysis (EPMA), X-ray photoelectron spectroscopy (XPS), thermogravimetric analysis (TGA), and differential scanning calorimetry (DSC). Cross-sectional analysis with EPMA of activated coke particles revealed that sulfur-rich coke particles (i.e., SIAC) could be produced with and without O₂. Under low SO₂ (3%), high O₂ (18%) conditions, however, O₂ competitively reacted with coke at 600 °C, and SO₂ only reacted to form a sulfur-rich layer after O₂ had been depleted. Analysis with XPS suggested that the sulfur-rich layer of the coke particles was made up of thiophene from the coke plus carbon–sulfur surface complexes, mainly heterocyclic sulfide and disulfide, while the presence of aliphatic sulfide, thiolactone, and thiol could not be ruled out. TGA and DSC analyses confirmed that sulfur added to activated coke via reaction with SO₂ was not elemental in nature. In both N₂ and air, sulfur added via high-temperature reaction with SO₂ is more thermally stable than that of a commercial SIAC sulfurized at lower temperatures. This may have beneficial implications if these SO₂ activated cokes were to be used to capture mercury, since they could be thermally regenerated with minimal loss of active sulfur surface sites while the captured mercury is collected, avoiding the costly and potentially problematic landfill disposal of Hg-containing activated carbon.

Introduction

Oil-sands fluid coke is a type of petroleum coke produced during the upgrading of Alberta oil-sands bitumen. It has high carbon (~85 wt %) and low ash (~5 wt %) contents, giving it a high heating value. However, oil-sands fluid coke is also rich in sulfur (~6 wt %), meaning that combustion to produce electricity would necessitate the use of expensive sulfur dioxide (SO₂) control equipment. For this reason, it is currently being stockpiled on-site at a rate of more than 10 000 ton/day. Efforts to find alternative uses for oil-sands fluid coke are underway, and one of its potential applications is in the reduction of SO₂ to elemental sulfur.

Previous research has shown that oil-sands fluid coke can be used to reduce SO₂ and produce elemental sulfur (S) as a coproduct at temperatures up to 1000 °C following reaction 1.¹



At 700 °C, complete SO₂ reduction occurred while elemental S yield peaked at approximately 95%. It was later determined that addition of oxygen (O₂) or water (H₂O) enhance the reduction of SO₂ by up to 15% due to the generation of carbon monoxide (CO) and hydrogen (H₂), which act as secondary reducing gases.²

* To whom correspondence should be addressed. Phone: +1 416 946 3097. Fax: +1 416 978 8605. E-mail: cq.jia@utoronto.ca.

[†] E-mail: eric.morris@utoronto.ca.

[‡] E-mail: kzmorita@iis.u-tokyo.ac.jp.

Another potential use for oil-sands fluid coke is the production of sulfur-impregnated activated carbon (SIAC). SIACs are typically produced from low-sulfur starting materials by several methods including direct sulfur deposition^{3–11} as well as reaction with sulfur gases such as H₂S,^{3,4,12–14} CS₂,^{3,4} and SO₂.^{3,4,13} It has also been found that the same reaction by which petroleum coke reduces SO₂ to elemental S (reaction 1) also physically activates the coke by producing a porous structure. SIACs of up to 360 m²/g have been produced in this manner.¹⁵ The usefulness of SIACs stems from the fact that carbon–sulfur surface complexes provide effective binding sites for removal of contaminant species. Several studies^{5–11,14} have indicated that SIACs are particularly well-suited for capturing vapor-phase mercury. However, these studies have not addressed the issue of mercury recovery and carbon regeneration after capture—it is typically assumed that the SIAC loaded with mercury will be treated as a hazardous waste and sent to landfill, but this has the obvious drawback of high material and handling costs. The ability to regenerate SIAC would therefore be economically beneficial while reducing its environmental burden. Thermal regeneration is the most commonly used technique for activated carbons; however, in the case of SIACs, the high temperatures used could also destroy the important sulfur sites on the carbon surface. Thus, it is vital that sulfur be impregnated in a way that imparts high-temperature stability to the carbon–sulfur groups if thermal regeneration of SIACs is to be done.

Bejarano et al.¹⁶ undertook a cross-sectional analysis of a single particle of oil-sands fluid coke after reaction with 15%

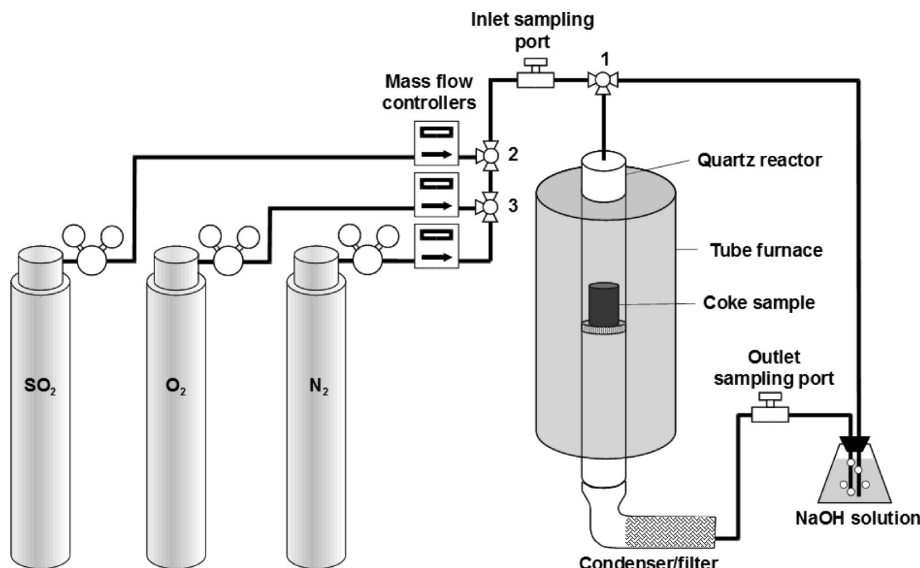


Figure 1. Schematic diagram of SO_2/O_2 –coke reaction apparatus. Three-way stopcocks are indicated at positions 1, 2, and 3.

SO_2 for 13 h using scanning electron microscopy with electron dispersive X-ray spectroscopy (SEM-EDX). An accumulation of sulfur was observed in between a mineral-rich ash layer and the unreacted core of the particle, similar to the sulfur-rich layer previously reported by Panagiotidis et al.¹⁷ for the reaction of anthracite char with SO_2 . Previous research has found that high-temperature reaction of SO_2 with a carbon surface may add sulfur in the form of sulfide,^{3,18} disulfide,¹⁸ thiol,³ thioketone,^{3,4} thiolactone (defined as a lactone with both oxygen atoms replaced by sulfur),⁴ and oxidized forms such as sulfones and sulfoxides,¹⁸ but not as elemental sulfur. Moreover, a large portion of the added sulfur was determined to be stable in N_2 at temperatures exceeding 700 °C,^{3,4} suggesting that thermal regeneration of SIACs produced through reaction with SO_2 might be feasible.

This investigation was intended to improve the current understanding of the reduction of SO_2 using oil-sands petroleum coke through analysis of the speciation and thermal stability of sulfur added to the coke surface through this process. Many real industrial stack gases for which SO_2 is a problem also contain high levels of O_2 ; therefore it is important to know what effect this has on coke particles if they are to be directly applied for SO_2 control. For this reason, a third goal of this investigation was to analyze how the SO_2 –coke reaction is impacted by a large excess of O_2 . In carrying out these objectives, a combination of microscopic elemental mapping of particle cross-sections and X-ray photoelectron spectroscopy (XPS) was utilized. Stability of sulfur on the activated coke surface was analyzed using XPS as well as thermogravimetric analysis (TGA) and differential scanning calorimetry (DSC).

Experimental Section

Sample Preparation. Raw fluid coke was obtained directly from an industrial bitumen upgrading facility and sieved to a particle size range of 212–300 μm . Approximately 10 g were weighed and placed on a fritted disk located at the midpoint of a quartz tube reactor 68 cm in length and 2.0 cm inner diameter (Figure 1). This resulted in a cylindrical coke bed of height 2.4 cm and volume 7.5 cm^3 , respectively. The entire reactor was suspended vertically within a tubular furnace (Carbolite), and the inlet and outlet attached to PVC tubing via ball-and-socket adapters sealed with vacuum grease. The outlet adapter was a

25 cm tube stuffed with quartz wool which acted as a condenser and filter for elemental sulfur produced in the reactor. Other gaseous products were removed using a sodium hydroxide scrubbing solution prior to venting.

Gases were supplied by cylinders (N_2 and O_2 at 99.995%, SO_2 at 99.3%) and their flow rates controlled by mass flow controllers (Aalborg). Each mass flow controller had previously been calibrated using a bubble flowmeter (Humonics). Gases were mixed to the desired concentrations by combining streams using Teflon three-way stopcocks. The total gas flow rate used was 200 cm^3/min , which is beyond the range in which external mass-transfer effects are expected to be significant.¹ A flow of pure N_2 was used to flush out the reactor for at least 15 min and was then maintained as the furnace was heated to the desired reaction temperature. After the temperature stabilized for 10 min, N_2 flow was diverted around the reactor using a three-way stopcock and SO_2 and/or O_2 was introduced. The concentrations of these gases were monitored by taking samples from the inlet sampling port with a gastight syringe and analyzing them using a Varian 3800 gas chromatograph (GC). This device was equipped with a molecular sieve 5A capillary column arranged in parallel with a porous divinylbenzene capillary column, both of which were 30 m in length and 0.53 mm inner diameter. After the gas concentrations stabilized, the gas mixture was introduced to the sample in the reactor for a period of 3 h. During this time, outlet gases were monitored with GC via the outlet sampling port. In this semibatch reactor, properties of the coke bed (mass and porous structure) were constantly changing with time as a result of reactions with O_2 and/or SO_2 . It is therefore impossible to reach a true steady state. However, the change in gas composition was observed to be relatively small during the sampling period. At the end of the experiment, SO_2 and/or O_2 were immediately shut off and N_2 was allowed to flow through the reactor until it had cooled sufficiently.

The product coke was not homogeneous due to the inequality in reaction rate from the top to the bottom of the bed, which was evident from the existence of a visible ash layer on the top. To analyze the different regions of the bed separately, coke was removed from the reactor in four roughly equal layers. This was done by means of suction using an aspirator and a narrow glass tube with a fritted glass filter. Care was made to maintain distinct layers; however, some degree of mixing inevitably

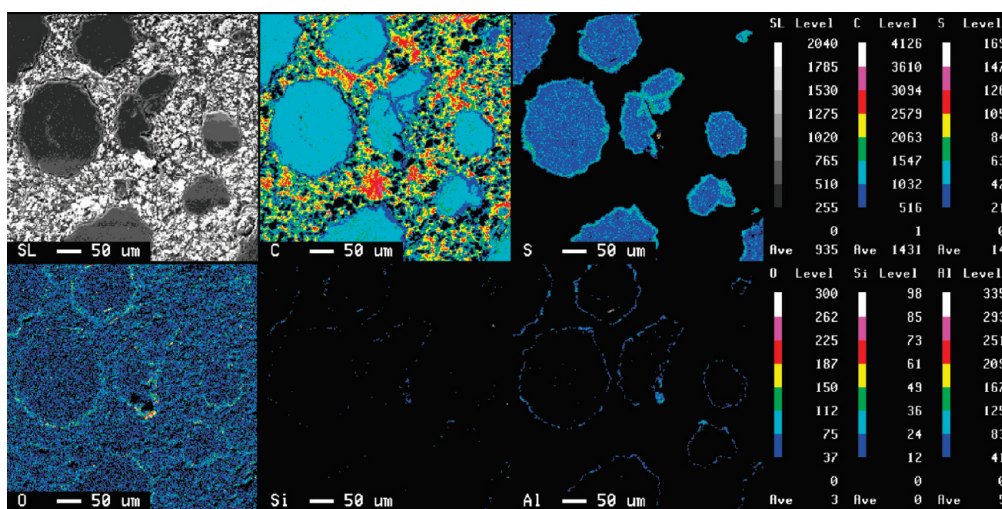


Figure 2. Wide-field WDX cross-sectional map for the upper layer of sample FC800. The color bars at right indicate relative signal intensity; concentrations were not quantified.

occurred. These layers were each weighed and then totaled to determine coke burnoff.

Two different samples derived from oil-sands fluid coke were used in this investigation: FC600 and FC800. FC800 was reacted with 30% SO₂ at 800 °C for 3 h, representing conditions under which high SO₂ reduction and sulfur fixation have been achieved in previous experiments. FC600 was made using 3% SO₂ combined with 18% O₂ at 600 °C for 3 h. These gas conditions were chosen to replicate those of a particular nonferrous metallurgical smelter flue gas, with a somewhat lower temperature to limit burnoff in the presence of O₂.

Sample Analysis. Treated particles from the uppermost layer of the coke bed were deposited at the bottom of 25 mm i.d. polyethylene casts. A cold-curing resin was then prepared and carefully poured over the particles to create a cylindrical cast. A conductive copper resin was initially used for this purpose but was later changed to a transparent epoxy resin for practical reasons. It is believed that the choice of resin material had insignificant effect on the analytical results. After 24 h setting time, casts were removed and polished using silicon carbide abrasive discs and 3 μm diamond water. Samples cast in epoxy were then carbon coated prior to being analyzed using a JEOL JXA-8900 SuperProbe electron probe microanalyzer (EPMA). This device used four different diffracting crystals (thallium acid phthalate (TAP), pentaerythritol (PETH and PETJ, where H and J are specifications used by JEOL), and layered dispersive element (LDE)) and scanning electron microscopy—wavelength dispersive X-ray spectroscopy (SEM-WDX) to produce two-dimensional elemental maps of the coke particle cross-sections. No quantitative analysis was performed with EPMA due to a lack of suitable standard materials.

X-ray analyses were performed using a Thermo Scientific K-Alpha XPS spectrometer using a monochromated aluminum X-ray beam and an electron flood gun to avoid charge build-up on the sample surface. The beam width used in all experiments was 400 μm. High-resolution scans of the sulfur 2p region were recorded to understand changes in the sulfur electron environment. Using Thermo Avantage software, each spectrum was calibrated with respect to the C 1s peak, and the S 2p_{1/2} and S 2p_{3/2} peaks were separated by exactly 1.18 eV.

TGA and DSC experiments were carried out simultaneously using a TA Instruments SDT Q600. Approximately 20 mg of sample was heated from room temperature to 950 at 10 °C/

min. This was done under pure N₂ and air for samples FC600, FC800, and a commercial SIAC, Calgon Carbon HGR. The exact method of sulfur impregnation for HGR is proprietary, but it results in a thin, uniform coating of elemental sulfur over the entire exterior and interior surface of a bituminous coal-based activated carbon.¹⁹ This material therefore provides a useful reference in determining the nature and stability of sulfur on the surface of SO₂-treated fluid coke.

Total sulfur content was determined using an Exeter Analytical CE-440 elemental analyzer. It should be noted that this device utilizes a combustion technique; thus, some forms of sulfur, such as inorganic sulfates and pyrite, are not accounted for. For this reason, sulfur contents determined using this method are referred to as “combustible sulfur”.

Results and Discussion

Characterization of Sulfur on Coke Activated with SO₂. Figure 2 shows a wide-field secondary electron image (SL) and EPMA elemental maps of C, S, O, Si, and Al for a sample from the upper layer FC800. The high background signal for C and O are due to the organic nature of the resin used in casting. This image reveals that particles within the upper layer of the coke bed were highly similar in terms of physical structure in that they all possess outer rings depleted of C but enriched with S, O, Si, and Al.

Upon closer examination, these particles were found to be surrounded by two distinct layers: a sulfur-rich layer around the unreacted core and an ash layer outside of this enriched with O, Si, and Al. A single-particle elemental map from the same sample is shown in Figure 3. The outer ash layer is clearly visible as a ring surrounding the particle highly enriched in Al and O. Both C and S were also detected in this outer layer but in low amounts. Carbon is likely present as residual unburned carbon but may also exist as carbonates. Sulfur in the ash layer is in the form of sulfate bound to calcium or other alkali minerals, as this is the predominant form of sulfate in coals.^{20,21} A previous ash composition analysis indicates that the ash portion of oil-sands fluid coke initially contains a considerable amount of sulfate (Table 1).²²

In the sulfur-rich layer, both O and Al were slightly enriched compared to their average bulk concentration within the particle. The enrichment of O in this region suggests that sulfur is in a

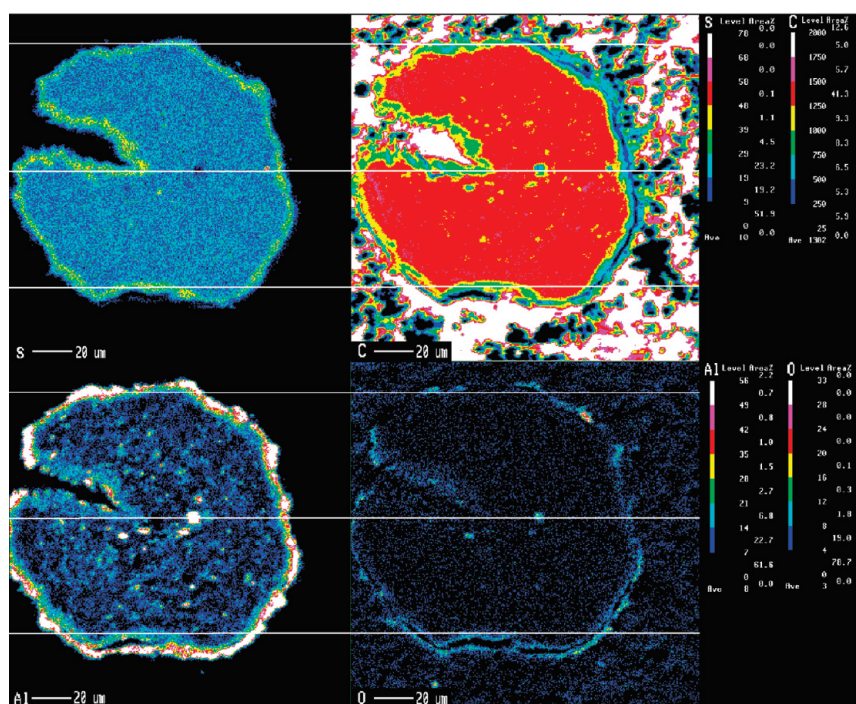


Figure 3. Single-particle WDX cross-sectional map for the upper layer of sample FC800. The color bars at right indicate the relative signal intensity. White lines are added as a vertical reference for comparison between different elements. C and Al color scales have been modified to enhance the contrast in low-concentration areas.

Table 1. Major Ash Components of Athabasca Oil-Sands Fluid Coke as Percent by Weight of Ash²²

component	1979–1980	1980–1982	1982–1983	1983–1985	1985–1996	average
SiO ₂	38.80	50.06	41.60	41.26	37.64	41.87
Al ₂ O ₃	24.35	20.94	24.22	24.94	24.23	23.74
Fe ₂ O ₃	9.72	8.18	9.26	12.14	11.42	10.14
V ₂ O ₅	4.46	3.20	4.86	3.21	4.94	4.13
TiO	3.64	2.86	3.25	4.84	4.63	3.84
CaO	4.26	2.58	4.20	1.63	2.94	3.12
SO ₃	3.59	2.73	2.65	1.87	2.88	2.74
K ₂ O	1.83	1.78	1.83	1.93	1.72	1.82
MgO	1.62	1.29	1.44	1.40	1.46	1.44
Na ₂ O	1.51	1.17	1.57	1.16	1.67	1.42
NiO	1.08	0.80	1.16	0.82	1.24	1.02

partially oxidized state, possibly due to interactions between SO₂ with basic minerals such as calcium oxide, according to



Bejarano et al.¹⁶ made similar observations of a sulfur-enriched layer for a sample made under similar conditions, attributing the accumulation to carbon surface sulfur complexes. Figure 3 indicates that the S-rich layer is 5–10 μm in thickness, however, which is too thick to be attributed to a single monolayer of surface groups. The only way this would be feasible is if the C–S surface complexes were bound to a highly porous carbon substrate, giving a high sulfur signal over a wide region. Carbon was highly depleted in this layer but still present in low concentrations, which indicate a highly developed porous structure. This scheme could also help to explain how sulfur, which vaporizes at 445 °C, could be stabilized during the reaction at 800 °C. Measurements of combustible sulfur content before and after the reaction with 30% SO₂ indicated an increase of approximately 3.8% (6.6 ± 0.3% initially, 10.4 ± 0.3% after treatment), suggesting a high degree of surface coverage by carbon–sulfur complexes in this region.

The XPS S 2p scan of sample FC800 is shown in Figure 4. The 2p binding energies for various sulfur compounds are well-

established and have been used in previous works to determine sulfur speciation in petroleum cokes and heavy petroleum residuals.^{4,18,23–26} Intensity peaks for oxidized sulfur forms appear at higher energy than do peaks for reduced forms; therefore, the leftmost peak in Figure 4 can be attributed to highly oxidized species such as sulfate. Since electrons detected by XPS originate from the outer 10 nm or so of the sample surface, this peak is most likely a result of sulfate species in the outer ash layer such as CaSO₄ (169.0 eV²⁷), while the small signal in the center could be from sulfites such as CaSO₃ (166.7 eV²⁸). Using petroleum coke from the same batch as the current

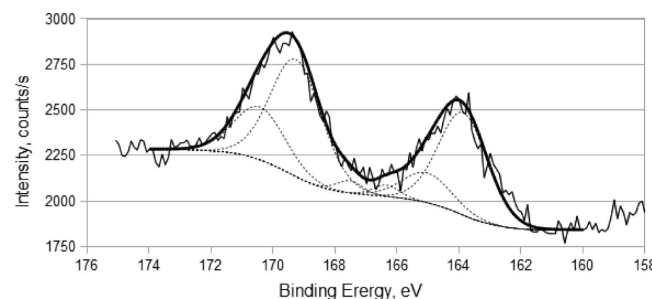


Figure 4. XPS S 2p spectrum for sample FC800: petroleum coke treated with 30% SO₂ at 800 °C for 3 h.

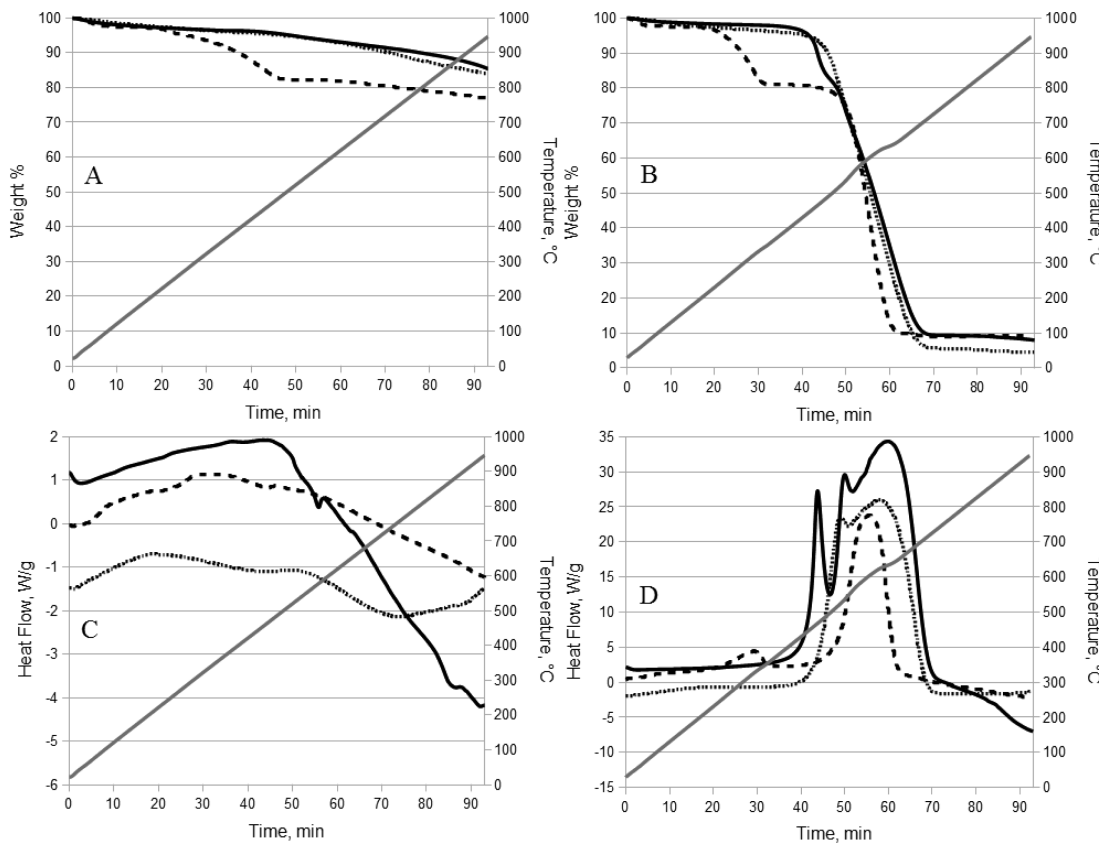


Figure 5. (A) TGA under N_2 , (B) TGA under air, (C) DSC under N_2 , and (D) DSC under air for FC800 (—), FC600 (···), and Calgon HGR (---). Temperature profile shown as a gray line.

study, Cai et al.²³ determined using XPS that sulfur on the raw coke surface was comprised of 5% sulfate and 4% sulfoxide. While sulfoxide groups may provide an alternative explanation for the small peak at ~ 166.4 eV, the presence of sulfate in the original coke lends support to its assignment to the leftmost peak in Figure 4.

The rightmost peak indicates reduced sulfur forms, which are expected in the layers beneath the ash. Although the ash layer thickness was observed to be much greater than the effective penetration depth of XPS, it is not expected to surround every particle uniformly, which can be seen in Figure 3. Thus, the rightmost peak is attributed to sulfur forms in the S-rich layer. The placement of this peak at approximately 164.0 eV provides some evidence as to the nature of the S-rich layer. Although this peak coincides well with that expected for elemental S,²⁷ Puri and Hazra³ demonstrated that elemental sulfur is not likely deposited on a carbon surface through reaction of SO_2 . Therefore, this peak is attributed to a combination of reduced carbon–sulfur compounds. Cai et al.²³ found that sulfur on the raw petroleum coke surface was comprised of 90% thiophene and/or similar sulfide structures. Therefore thiophene (164.3 eV²⁷) from the original coke structure is likely a major contributor to this peak, along with thiophene and similar ring structure sulfides (163.8, thianthrene²⁹) produced through carbon–sulfur substitutions during reaction. Carbon–sulfur surface compounds that were likely added include disulfides (164.4 eV, diphenyl disulfide²⁷), aliphatic sulfides (163.4 eV, diphenyl sulfide⁴), and thiolactones (163.4 eV, 1,3-dithiolane-2-thione⁴). Thiol (163.1 eV, thiophenol³⁰) and thio-ketone (162.4 eV, thiobenzophenone²⁹) may also be present, but evidently in smaller amounts.

Figure 5 shows TGA and DSC analyses in N_2 and air for FC600 and FC800 (taken from the top portion of the bed) as

well as Calgon HGR, which was determined to have a combustible sulfur content of $17.3 \pm 0.6\%$. From what is known about the sulfur impregnation technique of HGR, it is assumed that virtually all of this sulfur is elemental. HGR exhibited a mass decrease of approximately 16% between 200 and 500 °C in N_2 and 17% between 250 and 350 °C in air, both of which correspond well with the measured sulfur content. The loss is therefore attributed to complete volatilization of this sulfur from the surface in N_2 and rapid combustion of sulfur at its autoignition temperature of 250 °C in air. The TGA profiles for FC800 did not show a similar step, verifying that sulfur in the S-rich layer is not in elemental form.

Effect of O_2 Combined with SO_2 on S Distribution. A wide-field EPMA map of sample FC600 revealed a mixture of different types of particles in the upper layer of the coke bed (Figure 6). Some particles showed an outer sulfur layer such as those in Figure 1 (particle A), some exhibited outer ash layers of varying thicknesses (particles B and C), while others were simply ash (particles D and E). In Figure 6, the high carbon background signal from the resin reduces the contrast between ash and unreacted coke, which is why particles B and C appear to have similar carbon concentrations as particles D and E. In addition, particle A appears to have been located within a surface depression of the resin cast, which may account for its lower observed carbon concentration. The ash particles come from a light-colored region at the top of the bed and were formed at the upper surface of the coke bed by O_2 competitively reacting with carbon. Only after O_2 was used up did SO_2 react with coke, forming a S-rich layer near the coke surface. Over time, the O_2 reaction zone migrated downward through the coke bed as carbon was spent, consuming the S-rich layer in the process. This process is illustrated in Figure 7. SO_2 reacts much more slowly than O_2 and thus began to break through as the depth of

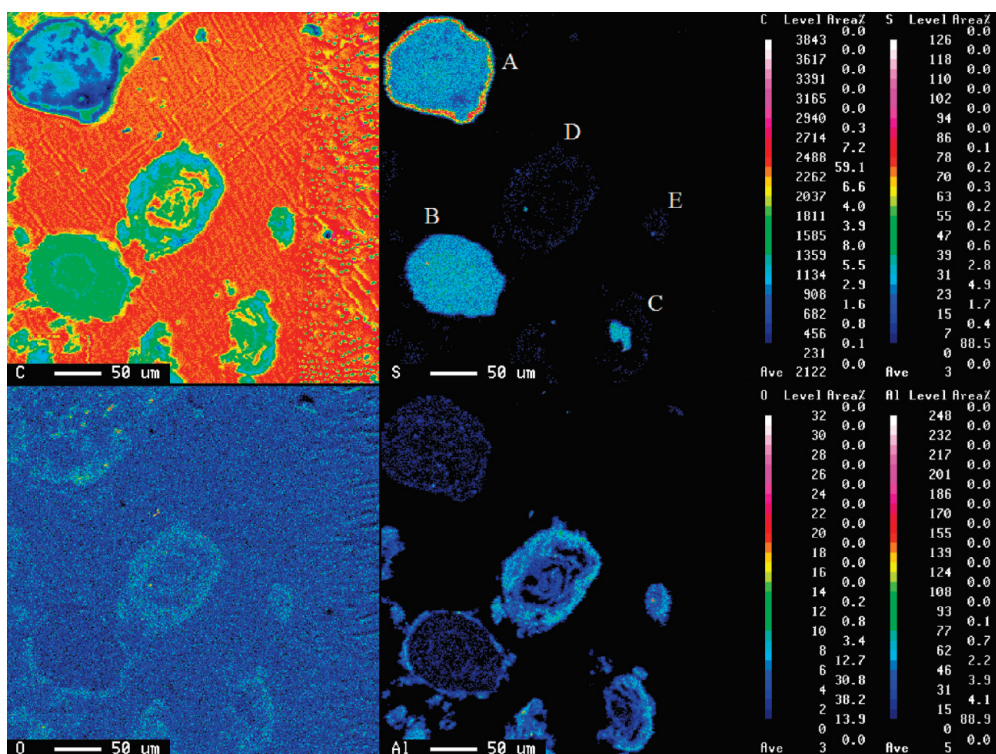


Figure 6. Wide-field WDX cross-sectional map for the upper layer of sample FC600. Color bars at right indicate relative signal intensity. Labels in sulfur map: (A) particle with outer S-rich layer; (B, C) particles with outer ash layer; (D, E) particles converted completely to ash.

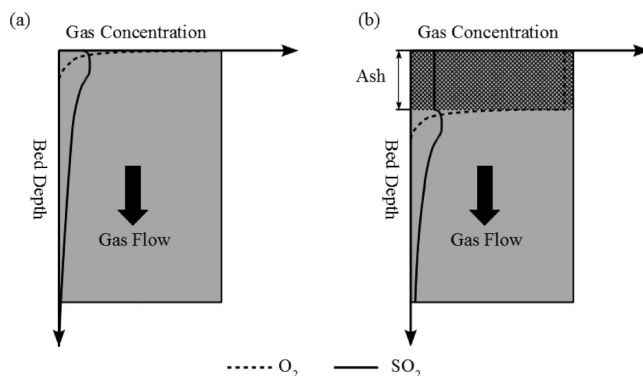
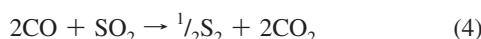


Figure 7. SO₂ and O₂ concentrations as a function of fixed bed depth for sample FC600 during (a) initial stages and (b) later stages of reaction. SO₂ initially increases slightly due to combustion of sulfur in coke. Not drawn to scale.

the reactive carbon bed decreased and the reactive residence time of SO₂ was reduced. This was observed experimentally using GC to monitor the effluent gases (Figure 8). While O₂ was completely removed, SO₂ broke through the bed after about 30 min and its outlet concentration appeared to increase gradually with time. The time needed for inlet gases to flow through the system was calculated as being slightly under 3 min; therefore the delayed appearance of SO₂ is not simply a result of space filling. Feng and Jia² observed a ~20% increase in SO₂ reduction with the addition of 18% O₂ at 700 °C, which was attributed to generation of CO according to



CO was not detected in the outlet gas stream during the production of sample FC600. Since residual SO₂ existed in

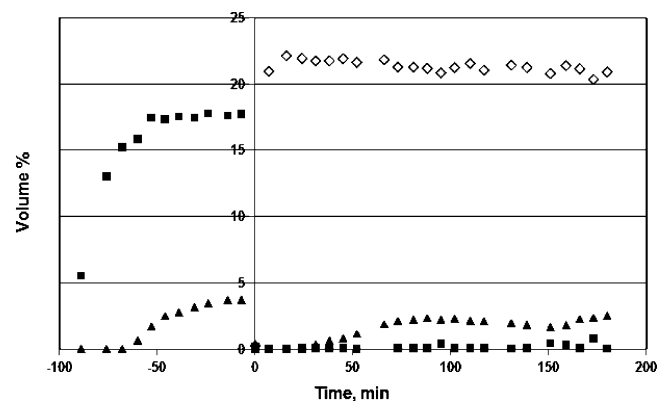


Figure 8. GC profile for sample FC600 showing O₂ (■), SO₂ (▲), and CO₂ (◊). Profiles before time = 0 represent stabilization of inlet gas concentrations prior to reaction with coke.

the outlet gas, reaction 3 was likely kinetically limited under the reaction conditions used.

Figure 9 provides a closer look at a single particle which is of the same type as particle A in Figure 6. It can be seen that the S-rich layer formed under these conditions was similar to that of FC800 in that carbon is depleted but still present, indicating a porous carbon layer. However, unlike with FC800, there is no ash layer surrounding the particle. This is attributed to the much lower SO₂ concentration that was used, as well as the lower reaction temperature, that led to reduced SO₂–C reactivity. Less reactive carbon forms which made up the porous carbon structure are not highly susceptible to attack by SO₂ under these conditions and remained intact throughout the reaction, thus precluding the formation of a separate ash layer. It is also evident that some areas of the S-rich layer are oxygen-deficient (upper left edge) while others are oxygen-rich (lower left and right edges). As with sample FC800, this can be attributed to the reaction of SO₂ with basic minerals inherently

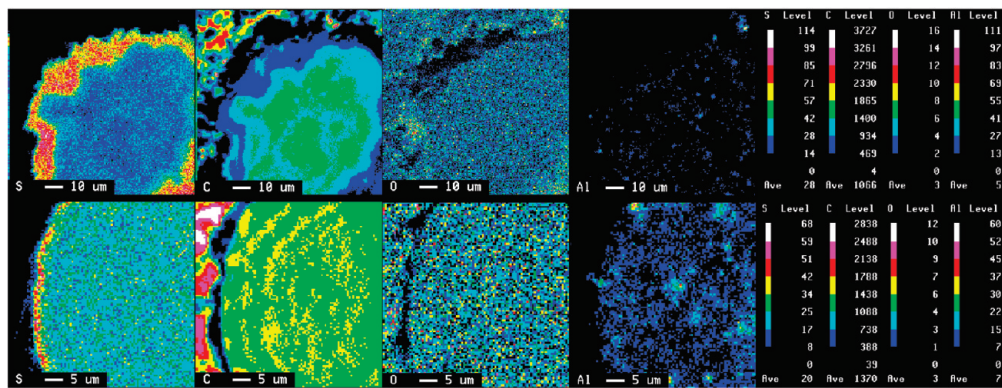


Figure 9. Single-particle WDX cross-sectional map for the upper layer (top row) and the lower layer (bottom row) of sample FC600. Color bars at right indicate relative signal intensity.

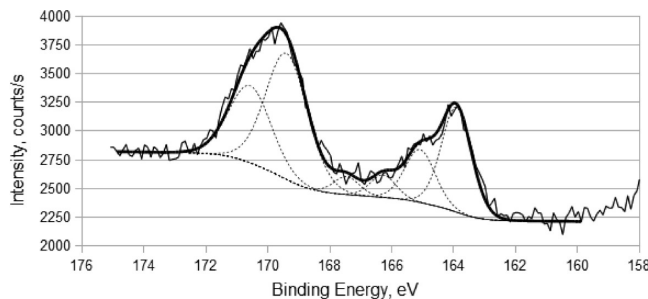


Figure 10. XPS S 2p spectrum for sample FC600: petroleum coke treated with 3% SO_2 + 18% O_2 at 600 °C for 3 h.

present in the coke to produce sulfites. Figure 9 also shows a particle extracted from the lower portion of the coke bed, which displays a relatively thin layer of sulfur enrichment. This lends further support to the scheme shown in Figure 7.

Figure 10 shows the XPS S 2p spectra for sample FC600. As with sample FC800, the leftmost peak is located at approximately 169.5 eV and therefore partially attributed to sulfate species such as CaSO_4 which are present in the ash particles. The fact that this peak is substantially larger for sample FC600, however, suggests another source of oxidized sulfur. It is conceivable that residual O_2 may persist into the SO_2 reaction region of the coke bed, which could oxidize existing carbon–sulfur compounds or produce carbon–oxygen surface complexes which subsequently react with SO_2 . In either case, the end result could be oxidized carbon–sulfur compounds such as sulfone or sulfonate.

Also similar to FC800, the reduced sulfur peak is positioned at approximately 164.0 eV and can therefore be attributed to a mixture of thiophene and reduced sulfur surface complexes, mainly disulfide, sulfide, and thiolactone. Significant differences between the reduced sulfur forms of FC600 and FC800 could not be detected using XPS. This similarity indicates that their S-rich layers were formed by a similar process despite the different gas conditions. Thus, although O_2 in the reactive gas stream clearly outcompetes SO_2 in the reaction with coke, the O_2 –carbon and SO_2 –carbon reactions seem to occur independently in separate regions of the coke bed as illustrated in Figure 7.

Humeres et al.³¹ used XPS to analyze a commercial activated carbon reacted with 20% SO_2 at 630 °C and detected peaks indicating the presence of S(IV) and S(II), but not S(VI). A mechanism was thus proposed in which SO_2 reacts at the surface to form dioxathiolane (S^{2+}) and sultine (S^{4+}) surface groups, which coexist alongside their decomposition product, episulfide

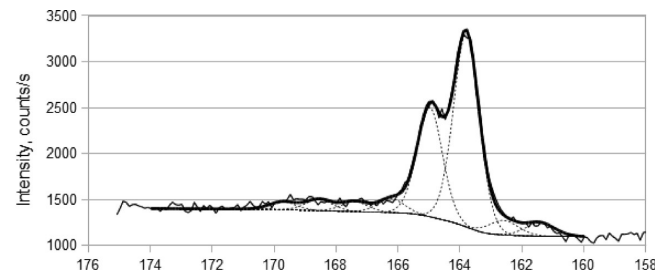


Figure 11. XPS S 2p spectrum for sample FC600 after heating in Ar at 800 °C for 1 h.

(S^{2+}).³² The data presented in Figure 10 do not preclude the existence of this mechanism.

Thermal Stability of Sulfur on Oil-Sands Fluid Coke Treated with SO_2 and O_2 . Sample FC600 was heated in a stream of pure argon at 800 °C for 1 h to determine how its sulfur content and speciation change upon heating in an inert atmosphere. Measurements of combustible sulfur content before and after the heating indicated a decrease of approximately 0.5% ($9.6 \pm 0.1\%$ before heating, $9.1 \pm 0.1\%$ after heating), suggesting that the combustible sulfur in the coke treated with SO_2 and O_2 was relatively stable during heating. Thermal stability is essential to the regeneration of spent SIAC.

The XPS S 2p spectrum for the heat-treated sample is shown in Figure 11. The most striking feature of this spectrum upon comparison with that of FC600 is the much smaller oxidized sulfur peak. Since the dominant source of oxidized sulfur in the original sample is thought to be metal sulfates in the ash particles, the lack of this peak indicates that sulfate is reduced upon heating in an inert atmosphere. Although the reduction of sulfate by solid carbon is thermodynamically feasible, the most likely reducer is CO gas which has been identified in the exit gas when fluid coke is heated under inert conditions. As shown in Figure 6, FC600 contains particles that were mostly unreacted with only a thin ash layer (particle B). Thus, it is likely that some pyrolysis of unreacted coke did occur. CO reduction of sulfate has been studied previously,^{33,34} and the following reaction has been proposed:



In the presence of catalysts such as Fe_2O_3 ^{33,34} and V_2O_5 ,³³ reaction 5 has been found to be feasible at temperatures as low as 600 °C. These transition metal oxides are known to exist in oil-sands fluid coke (see Table 1). Figure 11 also shows some evidence of metal sulfide species in the small $\text{S} 2p_{3/2}$ peak

located at approximately 161.4 eV, which agrees well with previously found S 2p_{3/2} binding energy for CaS of 161.0 ± 0.2 eV.³⁵

As shown in Figure 5A, TGA profiles for samples FC600 and FC800 in N₂ did not exhibit the same step decrease in mass attributed to loss of elemental sulfur in the case of HGR. However, there was an overall weight loss of approximately 15% observed in both samples which gradually accelerated with increasing temperature. In addition to CO pyrolysis of the coke and reduction of oxidized sulfur, the loss of sulfur groups added during reaction with SO₂ is also partially responsible.

Figure 5B shows the TGA profiles in a stream of air. The step decrease attributed to combustion of elemental sulfur at 250 °C for HGR has a corresponding peak in the HGR DSC curve (Figure 5D). This was not observed for FC600 or FC800; however, FC800 does exhibit a strongly exothermic reaction feature at ~400 °C, which appears just before the carbon combustion peak. This can be explained as the combustion of sulfur which is liberated from the S-rich layer as its porous carbon substrate is consumed. This peak is absent from the FC600 DSC curve; evidently, the FC600 sample which was heated in air contained very few if any particles with an S-rich layer.

The DSC profile for FC800 in N₂ (Figure 5C) shows a small feature at approximately 575 °C which does not have a corresponding feature on the TGA curve. This DSC feature was not observed for FC600 in N₂. In air, however, both FC600 and FC800 exhibited a peak that is highly similar (Figure 5D). The reason(s) behind these observations are not clear at this stage. A TGA-MS analysis may help find an explanation.

TGA analysis verifies that sulfur added to carbon through high-temperature reaction with SO₂ is more thermally stable in both N₂ and air than sulfur added by direct condensation at lower temperatures. Puri and Hazra³ and Humeres et al.¹⁸ indicated that much of the sulfur added by this technique was in the form of heterocyclic ring structures such as thiophene and that these structures are highly stable at elevated temperatures (>700 °C) under inert conditions. SIACs made using this technique might therefore be economically beneficial to mercury-emitting industries, as the active sulfur sites which aid in capturing mercury would not as easily be removed upon heating. This would allow for thermal regeneration of the SIAC to collect the mercury and avoid the costly alternative of shipping the spent carbon to a hazardous waste landfill.

Conclusions

In this work, the effect of oxygen on the characteristics of SIAC produced by the high-temperature SO₂ process was studied. The following conclusions can be drawn.

(1) With SO₂ as the lone oxidizer, the high-temperature (800 °C) SO₂ process was able to produce SIAC. Although elemental sulfur was the major product of carbothermal reduction of SO₂, the high temperature had prevented elemental sulfur from depositing on the coke. However, a substantial amount of sulfur, in forms other than elemental sulfur, was enriched in the activated coke.

(2) The enriched sulfur was made up of thiophene from the raw coke plus carbon–sulfur surface complexes from carbon–SO₂ reactions. These complexes included mainly heterocyclic sulfide/disulfide, possibly aliphatic sulfide, thiolactone, and thiol. TGA and DSC analyses confirmed that sulfur added to coke via reaction with SO₂ was not elemental in nature.

(3) When both SO₂ (3%) and O₂ (18%) were present in the gas phase, the petroleum coke reacted with O₂ preferentially.

The reaction between the coke and O₂ gasified the coke, left behind ash, and prevented the enrichment of sulfur in the coke. Upon depletion of O₂, carbothermal reduction of SO₂ kicked in and resulted in sulfur enrichment in activated coke. Consequently, the treated coke in the fixed bed reactor was made up of a mixture of particles: completely ashed, partially ashed, sulfur-enriched, and unreacted.

(4) XPS analysis could not detect significant differences between the sulfur-rich particles produced with and without O₂, except for the possible presence of oxidized sulfur forms under high O₂ conditions.

(5) Analysis with XPS suggested that sulfur in ash was mainly composed of sulfates.

(6) In both N₂ and air, sulfur added via high-temperature reaction with SO₂ was more thermally stable than that of a commercial SIAC sulfurized at lower temperatures. Upon heating (to 800 °C) in an inert atmosphere, much (83%) of the sulfur added with SO₂ remained in the coke, while virtually all of the impregnated sulfur was lost from the commercial SIAC. This may have beneficial implications if these SO₂-treated cokes were used to capture mercury from flue gases, since they could be thermally regenerated with minimal loss of active sulfur surface sites, avoiding the costly landfill disposal of mercury containing activated carbon.

Acknowledgment

For financial support, we thank the Consortium of Sustainable Materials (COSM), a working partnership between the University of Tokyo and the University of Toronto, and NSERC. For their technical expertise and assistance, we thank Dr. Youngjo Kang and Motohiro Sakamoto of the University of Tokyo, and Dr. Sue Mao and Dr. Peter Brodersen of the University of Toronto.

Literature Cited

- Bejarano, C. A.; Jia, C. Q.; Chung, K. H. A Study on Carbothermal Reduction of Sulfur Dioxide to Elemental Sulfur Using Oilsands Fluid Coke. *Environ. Sci. Technol.* **2001**, *35*, 800.
- Feng, W.; Jia, C. Q. Influence of O₂ and H₂O on Carbothermal Reduction of SO₂ by Oil-Sand Fluid Coke. *Environ. Sci. Technol.* **2005**, *39*, 9710.
- Puri, B. R.; Hazra, R. S. Carbon-Sulphur Surface Complexes on Charcoal. *Carbon* **1971**, *9*, 123.
- Chang, C. H. Preparation and Characterization of Carbon-Sulfur Surface Compounds. *Carbon* **1981**, *19*, 175.
- Otani, Y.; Emi, H.; Kanaoka, C.; Uchijima, I.; Nishino, H. Removal of Mercury Vapor from Air with Sulfur-Impregnated Adsorbents. *Environ. Sci. Technol.* **1988**, *22*, 708.
- Korpel, J. A.; Vidic, R. D. Effect of Sulfur Impregnation Method on Activated Carbon Uptake of Gas-Phase Mercury. *Environ. Sci. Technol.* **1997**, *31*, 2319.
- Liu, W.; Vidic, R. D.; Brown, T. D. Optimization of Sulfur Impregnation Protocol for Fixed-Bed Application of Activated Carbon-Based Sorbents for Gas-Phase Mercury Removal. *Environ. Sci. Technol.* **1998**, *32*, 531.
- Liu, W.; Vidic, R. D.; Brown, T. D. Optimization of High Temperature Sulfur Impregnation on Activated Carbon for Permanent Sequestration of Elemental Mercury Vapors. *Environ. Sci. Technol.* **2000**, *34*, 483.
- Hsi, H.-C.; Rood, M. J.; Rostam-Abadi, M.; Chen, S.; Chang, R. Effects of Sulfur Impregnation Temperature on the Properties and Mercury Adsorption Capacities of Activated Carbon Fibers (ACFs). *Environ. Sci. Technol.* **2001**, *35*, 2785.
- Hsi, H.-C.; Rood, M. J.; Rostam-Abadi, M.; Chen, S.; Chang, R. Mercury Adsorption Properties of Sulfur-Impregnated Adsorbents. *J. Environ. Eng.* **2002**, *128*, 1080.
- Werner, M.; Heschel, W.; Wirling, J. Enhanced Adsorption of Elemental Mercury by Sulfurized Activated Lignite HOK, Presented at the

23rd Annual International Pittsburgh Coal Conference, Pittsburgh, PA, USA, Sep. 25–28, 2006.

(12) Sinha, R. K.; Walker, P. L., Jr. Removal of Mercury by Sulfurized Carbons. *Carbon* **1972**, *10*, 754.

(13) Valenzuela Calahorro, C.; Macias Garcia, A.; Bernalte Garcia, A.; Gomez Serrano, V. Study of Sulfur Introduction in Activated Carbon. *Carbon* **1990**, *28*, 321.

(14) Feng, W.; Borguet, E.; Vidic, R. D. Sulfurization of Carbon Surface for Vapor Phase Mercury Removal—I: Effect of Temperature and Sulfurization Protocol. *Carbon* **2006**, *44*, 2990.

(15) Chen, Y. Preparation, Characterization and Application of Novel Adsorbent from Petroleum Coke Activated by Sulphur Dioxide. MA.Sc. thesis, University of Toronto, Canada, 2002.

(16) Bejarano, C.; Jia, C. Q.; Chung, K. H. Mechanistic Study of the Carbothermal Reduction of Sulfur Dioxide with Oil Sand Fluid Coke. *Ind. Eng. Chem. Res.* **2003**, *42*, 3731.

(17) Panagiotidis, T.; Richter, E.; Junge, H. Structural Changes of an Anthracite Char during the Reaction with Sulphur Dioxide. *Carbon* **1988**, *26*, 89.

(18) Humeres, E.; Peruch, M. G. B.; Moreira, R. F. P. M.; Schreiner, W. Reactive Intermediates of the Reduction of SO₂ on Activated Carbon. *J. Phys. Org. Chem.* **2003**, *16*, 824.

(19) HGR for Mercury Removal. Calgon Carbon fact sheet. Calgon Carbon: Pittsburgh, PA, 2006; online, http://www.calgoncarbon.com/carbon_products/vapor.html, retrieved on April 12, 2010.

(20) Schafer, H. N. S. An Improved Spectrophotometric Method for the Determination of Sulfate with Barium Chloranilate as Applied to Coal Ash and Related Materials. *Anal. Chem.* **1967**, *39*, 1719.

(21) Goswami, U.; Baruah, M. K.; Haque, I. The Extraction of Sulfate Sulfur from Coals by Organic Acids. *Fuel Process. Technol.* **1999**, *58*, 103.

(22) Furimsky, E. Gasification of oil sand coke: Review. *Fuel Process. Technol.* **1998**, *56*, 263.

(23) Cai, J. H.; Morris, E.; Jia, C. Q. Sulfur Speciation in Fluid Coke and Its Activation Products Using K-Edge X-ray Absorption Near-Edge Structure Spectroscopy. *J. Sulfur Chem.* **2009**, *30*, 555.

(24) Kelemen, S. R.; George, G. N.; Gorbaty, M. L. Direct Determination and Quantification of Sulphur Forms in Heavy Petroleum and Coals. 1. The X-ray Photoelectron Spectroscopy (XPS) Approach. *Fuel* **1990**, *69*, 939.

(25) Jiménez Mateos, J. M.; Fierro, J. L. G. X-ray Photoelectron Spectroscopic Study of Petroleum Fuel Cokes. *Surf. Interface Anal.* **1996**, *24*, 223.

(26) Guo, Z.; Fu, Z.; Wang, S. Sulfur Distribution in Coke and Sulfur Removal during Pyrolysis. *Fuel Process. Technol.* **2007**, *88*, 935.

(27) Moulder, J. F.; Stickle, W. F.; Sobol, P. E.; Bomben, K. D. *Handbook of X-ray Photoelectron Spectroscopy*.: Perkin-Elmer: Eden Prairie, MN, 1992.

(28) Siriwardane, R. V. Interaction of SO₂ and O₂ Mixtures with CaO (100) and Sodium Deposited on CaO (100). *J. Colloid Interface Sci.* **1988**, *132*, 200.

(29) Brauman, S. K. Chemiluminescence Studies of the Low Temperature Thermooxidation of Poly(phenylene) Sulfide. *J. Polym. Sci., Part A: Polym. Chem.* **1989**, *27*, 3285.

(30) Roberts, J. T.; Friend, C. M. Spectroscopic Identification of Surface Phenyl Thiolate and Benzyne on Mo(110). *J. Chem. Phys.* **1988**, *88*, 7172.

(31) Humeres, E.; Peruch, M. G. B.; Moreira, R. F. P. M.; Schreiner, W. Reduction of Sulfur Dioxide on Carbons Catalyzed by Salts. *Int. J. Mol. Sci.* **2005**, *6*, 130.

(32) Humeres, E.; de Castro, K. M.; Moreira, R. F. P. M.; Peruch, M. G. B.; Schreiner, W. H.; Aliev, A. E.; Canle, M.; Santaballa, J. A.; Fernández, I. Reactivity of the Thermally Stable Intermediates of the Reduction of SO₂ on Carbons and Mechanisms of Insertion of Organic Moieties in the Carbon Matrix. *J. Phys. Chem. C* **2008**, *112*, 581.

(33) Zadick, T. W.; Zavaleta, R.; McCandless, F. P. Catalytic Reduction of Calcium Sulfate to Calcium Sulfide with Carbon Monoxide. *Ind. Eng. Chem. Process Des. Dev.* **1972**, *11*, 283.

(34) Li, H.; Zhuang, Y. Catalytic Reduction of Calcium Sulfate to Calcium Sulfide by Carbon Monoxide. *Ind. Eng. Chem. Res.* **1999**, *38*, 3333.

(35) Franzen, H. F.; Umaña, M. H.; McCreary, J. R.; Thorn, R. J. XPS Spectra of Some Transition Metal and Alkaline Earth Monochalcogenides. *J. Solid State Chem.* **1976**, *18*, 363.

Received for review June 29, 2010
Revised manuscript received September 20, 2010
Accepted October 18, 2010

IE101388Q